

Spectral weight function for the half-filled Hubbard model: a singular value decomposition approach

C.E. Creffield, E.G. Klepfish, E.R. Pike and Sarben Sarkar

Department of Physics, King's College London, Strand, London WC2R 2LS, UK

The singular value decomposition technique is used to reconstruct the electronic spectral weight function for a half-filled Hubbard model with on-site repulsion $U = 4t$ from Quantum Monte Carlo data. A two-band structure for the single-particle excitation spectrum is found to persist as the lattice size exceeds the spin-spin correlation length. The observed bands are flat in the vicinity of the $(0, \pi), (\pi, 0)$ points in the Brillouin zone, in accordance with experimental data for high-temperature superconducting compounds.

PACS numbers: 74.20.-z, 74.20.Mn, 74.25.Dw

The study of the normal properties of the high-temperature superconducting compounds and the attempts to construct a microscopic theory of superconductivity in these materials has been in large part dedicated to the investigation of the Fermi surface structure and its dependence on the strong electronic correlations and antiferromagnetic order. Angle-resolved photoemission experiments (ARPES) have recently provided a comprehensive mapping of the Fermi surface in some of the cuprates ($\text{YBa}_2\text{Cu}_4\text{O}_2$ and $\text{Bi}_2\text{Sr}_2\text{CaCu}_2\text{O}_{8+x}$)[1],[2],[3]. These results are particularly relevant to the high-temperature superconductivity scenario in which the phenomenon is related to the presence of van Hove singularities in the density of states close to the Fermi surface [1]. Quantum Monte Carlo simulations have recently been used to compare these experimental results with numerical calculations in models of strongly correlated electrons [4],[5]. An essential part of these numerical results was the extraction of the spectral weight function (SWF) for single-particle excitations from the Quantum Monte Carlo data calculated for imaginary time.

The SWF is obtained as a solution of the following inverse problem [7]:

$$G(\vec{k}, \tau) = \int_{-\infty}^{\infty} d\omega \frac{e^{-\omega\tau}}{1 + e^{-\omega\beta}} A(\vec{k}, \omega); \quad (0 < \tau \leq \beta) \quad (1)$$

where $G(\vec{k}, \tau)$ is the Matsubara Green's function for lattice momentum \vec{k} and imaginary-time separation τ , obtained in the finite-temperature Monte Carlo simulations at temperature $1/\beta$, and $A(\vec{k}, \omega)$ is the corresponding SWF.

This inverse problem admits an infinite class of solutions for $A(\vec{k}, \omega)$ which will satisfy Eq.(1) within small perturbations of the l.h.s., originating from the statistical noise on the simulation data. In recent works the one-electron SWF for the single-band 2D Hubbard model was obtained from Monte Carlo data using a maximum entropy approach [8],[9],[13]. The finite-size effects evident in the data itself, as well as in the reconstruction of the

SWF, led the authors of Ref.[8] to conclude that the pseudogap in the single-particle spectrum observed in small clusters (up to 8^2) is a lattice-size artifact which disappears as the size of the simulated system increases. They suggested therefore that for on-site repulsion weaker than the Hubbard bandwidth ($8t$) the antiferromagnetic correlation length would be comparable to the size of a sufficiently small lattice and would effectively create long-range antiferromagnetic order. Based on this conclusion the $U = 4t$ coupling (where U is the on-site Coulomb repulsion and t is the nearest-neighbour hopping parameter) was regarded as belonging to the weak-coupling regime, where the band structure is essentially similar to that of noninteracting electrons for all temperatures above zero, in accordance with the Mermin-Wagner theorem. Following this argument, a gap originating from spin-density waves (SDW) will be both temperature and finite-size sensitive. The low-temperature simulations, as presented in [10] for $\beta = 12$ show indeed a stable gap even for relatively large lattice size. Such temperature dependence of the gap would be expected to correspond to a strong temperature dependence of the spin-spin correlations. However, as the numerical results of Refs.[11] and [12] show, the spin-spin correlations at $U = 4t$ and 4^2 lattice fall rapidly within 2 lattice spacings with only minor dependence on the temperature in the range $\beta = 4 - 12$. The SWF presented in Ref.[8] shows a clear two-peak structure for this value of U and lattice linear dimension larger than the correlation length. Hence the possibility that the band structure is due to the short-range antiferromagnetic order (as was suggested in Ref.[3]) demands an accurate mapping of the on-site repulsion regimes for coupling $U < 8t$.

A detailed study of the SWF as a solution of an inverse problem requires a quantitative criterion for the resolution limits of the reconstruction technique. Without such a criterion an existing gap might be overlooked in the reconstruction procedure. Moreover, the single-particle spectrum derived from the distribution of the function $A(\vec{k}, \omega)$ along the Brillouin zone is based on the identifi-

cation of the peaks of this function. Thus the resolution of the two-peak structure, even if there is no clear evidence of the vanishing of this function between the peaks, is important.

In our work we use a method based on the singular value decomposition (SVD) approach widely used in the field of inverse problems [14]. This technique allows us to define the resolution limits quantitatively, thus providing an upper bound on the size of the gap with respect to the lattice size.

The work presented is an investigation performed on lattice sizes ranging between 4^2 and 12^2 . The simulation temperature was chosen as $\beta = 5$ and on-site repulsion as $U = 4t$. To avoid the sign problem the model was simulated at half-filling. However, the SVD treatment can be extended to finite doping, as well as to other Green's functions.

Eq.(1) can be rewritten in operator form as follows [14]:

$$G(\tau_i) = (\mathcal{K}A)(\tau_i). \quad (2)$$

\mathcal{K} is the integral operator of the r.h.s. of (1), with the variable τ in the kernel discretised, acting on the function A . This operator defines a transformation from the L^2 space of the SWF to the data space of which $G(\tau_i)$ is a vector. This transformation may be regarded as a rectangular matrix, \mathcal{K} , one of whose dimensions is infinite and the other equal to the dimension of the data space, namely to the number of data points n_τ . A conjugate operator \mathcal{K}^* acts in the data space and is determined by the following equality of inner products:

$$\sum_{i,j=1}^{n_\tau} W_{\tau_i \tau_j} (\mathcal{K}A)(\tau_i) G(\tau_j) = \int d\omega A(\omega) (\mathcal{K}^* G)(\omega), \quad (3)$$

with a metric tensor W which can account for the correlations in the data points. A common choice is to define this metric as the inverse of the covariance matrix [14]. The operator $\mathcal{K}\mathcal{K}^*$ is represented by a symmetric square matrix with a positive set of n_τ eigenvalues $\{\alpha_i^2\}$ and corresponding set of orthonormal eigenvectors $\{v_i\}$. These vectors form a basis in the data space. The operator $\mathcal{K}^*\mathcal{K}$ acting in the space to which the solution $A(\omega)$ belongs has a set of n_τ orthonormal eigenfunctions $\{u_i\}$ with the same eigenvalues. If the set $\{\alpha_i\}_{i=1}^{n_\tau}$ is arranged in descending order each vector v_k and function u_k will have $k - 1$ nodes. These two sets $\{u_i\}$ and $\{v_i\}$ and the set $\{\alpha_i\}_{i=1}^{n_\tau}$ form a singular system satisfying the equations:

$$\begin{aligned} \mathcal{K}u_k &= \alpha_k v_k \\ \mathcal{K}^*v_k &= \alpha_k u_k. \end{aligned} \quad (4)$$

The matrix representation of the operator $\mathcal{K}\mathcal{K}^*$ is obtained[14] from the kernel of Eq.(1) as:

$$(\mathcal{K}\mathcal{K}^*)_{\tau_m \tau_n} = \sum_{\tau_k} W_{\tau_m \tau_k} \int_{-\infty}^{\infty} d\omega \frac{e^{-\omega(\tau_k + \tau_n)}}{(1 + e^{\omega\beta})^2}. \quad (5)$$

The solution of Eq.(1) expanded in the functions $\{u_k\}$ is given by:

$$A(\omega) = \sum_{k=1}^{n_\tau} \frac{1}{\alpha_k} \langle G, v_k \rangle u_k(\omega) \quad (6)$$

where $\langle \cdot, \cdot \rangle$ denotes the inner product in the data space. The smallest singular values will greatly amplify the contribution of the statistical noise to the expansion coefficients in Eq.(6). We therefore introduce a cut-off into the expansion to exclude terms with $\frac{\alpha_k}{\alpha_1}$ smaller than the statistical error in $G(\tau)$ [15].

The “resolution ratio” depends on the number of nodes in the function with the highest index k_{max} included in the truncated expansion [16]. Here prior information about the support of the solution is essential. Since we assume that the $A(\omega)$ is localised within a certain range of ω , we confine the singular functions to this range. This is done by multiplying the kernel in Eq.(1) by a profile function which is approximately 1 within the support and smoothly vanishes outside it [16]. The rate of the decrease of the singular values for the limited support grows as the profile function gets tighter, therefore, the truncation in (6) will have a smaller k_{max} . However, since the support of the singular functions is limited, their nodes will be more closely spaced, thus giving better resolution. To investigate the resolution limits, artificial data was generated by substituting an $A(\omega)$ consisting of two Gaussian peaks into Eq.(1). The inverse problem was then solved for $A(\omega)$ with the expansion (6) truncated at $\frac{\alpha_1}{\alpha_k}$ exceeding a hypothetical noise level. Similar to the results of Ref.[16] we found that for a fixed noise the resolution improves as the range of support decreases.

The reconstruction of the SWF for \vec{k} at the vicinity of $\vec{k} = (\frac{\pi}{2}, \frac{\pi}{2})$ is given in Fig.1. It can be seen that there are negative side-lobes. Just as a positive δ -function, imaged over a limited Fourier bandwidth, turns into Airy rings which have negative side-lobes, we must expect a localised SWF, reconstructed over a limited singular function bandwidth, to have similar features. A regularization procedure which would restrict the solution to positive values only may also reduce the resolution of its reconstruction [15]. We present here the results of the 8^2 - 12^2 lattices, since the existence of the gap in the smaller lattices is beyond controversy. Limiting the support of $A(\vec{k}, \omega)$ to the range $[-8, 8]$, allowed us to identify a gap unseen in an infinite-support reconstruction. According to our statistical noise we truncated the expansion of $A(\vec{k}, \omega)$ with the ratio $\frac{\alpha_1}{\alpha_k}$ not exceeding 100 (for a 1% statistical error as estimated for 4000 Monte Carlo measurements) which allowed us to use 9 singular functions in the unlimited-support case and 7 in the reconstruction with the finite profile.

Since the statistical noise determines the level of truncation of the singular-function expansion it is clear that at a particular truncation level, not all the data included

in the n_τ points are of identical relevance. In accordance with the application of sampling theory in other inverse problems we identify as essential the nodes of the $v_{k_{max}}$. This is a generalisation of the Nyquist rate in Fourier theory. For example, in the inversion of the Laplace transform [17] the optimal sampling was found to be exponential which corresponds to the nodes of $v_{k_{max}}$. Application of this sampling technique to the inverse problem (1) is performed as follows: we estimate k_{max} from the knowledge of the noise and the spectrum of the singular values. Then the data is evaluated at points nearest to the nodes of $v_{k_{max}}$ and the SVD reconstruction is done for these points only. This procedure leads to an obvious advantage from the computational point of view, since the evaluation of the Matsubara Green's functions is reduced to $\frac{1}{5}$ of the total points. Moreover, by separating the data points by a large spacing we reduce the correlations within the data and the metric on the data space can be taken as Euclidean, which also substantially reduces the calculational effort. For the 8^2 lattice we evaluated the SWF using 7 data points only and compared the results with that obtained from using 40 equally spaced points. For the latter case we accounted for the correlations using the covariance matrix as the metric in the data space. The results show remarkable agreement, thus fully justifying the sampling approach in this problem.

In Fig.2 we present the density of states calculated for the three biggest lattice sizes as the solution $N(\omega)$ of:

$$\tilde{G}(0, \tau) = \int_{-\infty}^{\infty} d\omega \frac{e^{-\omega\tau}}{1 + e^{-\omega\beta}} N(\omega) \quad (7)$$

with $\tilde{G}(0, \tau)$ being the zero-space-separation Matsubara Green's function. In this reconstruction the range of the support for $N(\omega)$ is [-12, 12].

The gap decreases as the lattice size increases, in correspondence with the results of Vekić and White [8], but it is still clear even in the 12^2 lattice. In fact the difference in the size and depth of the gap is very small as the lattice size increases from 8^2 to 12^2 , while the linear dimension of the lattice is considerably larger than the SDW correlation length. The existence of two clear peaks in the density of states (as well as in $A(\vec{k}_{Fermi}, \omega)$) suggests a two-band structure of the spectrum.

The reliability of our results has been tested against the following criteria: the successful reconstruction of the Monte-Carlo data when the solution of $A(\vec{k}, \omega)$ is substituted in the r.h.s. of Eq.(1); the successful reconstruction of the same data by:

$$G = \sum_k^{k_{max}} \langle G, v_k \rangle v_k; \quad (8)$$

and, finally, by checking the first three moments of the SWF:

$$\mu_n = \int \omega^n A(\vec{k}, \omega) d\omega \quad (n = 0, 1, 2) \quad (9)$$

and the same moments for the density of states. We present in Table 1 the values of these moments for the density of states, showing excellent agreement with the analytic values 1, 0, 8 for the zeroth, first and second moments respectively [8].

lattice	μ_0	μ_1	μ_2
8^2	1.00	0.00	7.99
10^2	1.00	0.00	7.79
12^2	1.00	0.00	7.77

Table 1. The first three moments of the density of states versus lattice size.

Fig.3 shows the single-particle spectrum derived from identifying $E(\vec{k})$ as the location of a peak of $A(\vec{k}, \omega)$, where the values of the momentum \vec{k} scan over the Brillouin zone. In the calculation of the spectrum we observe a significant difference between the 8^2 and the 12^2 results. Both lattices exhibit a clear two-band structure of the single-particle spectrum. However, while the former can be fitted well with the mean-field SDW formula:

$$E(\vec{k})_{MF} = \sqrt{(\epsilon(\vec{k})^2 + \Delta^2)} \quad (10)$$

where $\epsilon(\vec{k}) = -2t(\cos k_x + \cos k_y)$ and $\Delta = 0.64t$, the 12^2 lattice shows a bigger gap at the corners of the noninteracting Fermi surface than at the point $(\frac{\pi}{2}, \frac{\pi}{2})$. Indeed the 12^2 lattice simulation gives a smaller gap at this point than the 8^2 and the 10^2 (see Fig.1). However, at the points $(\pi, 0)$ the gap remains persistently clear for all the lattices. This result can be interpreted as suggesting a gap due to an anisotropic pairing channel [2] (although not necessarily of $d_{x^2-y^2}$ symmetry). Higher resolution calculations, based on data with better statistics will be required to examine this possibility. We also observe the feature of a flat band near $\vec{k} = (\pi, 0)$ similar to the results of Dagotto *et al.*[4] and the experimental data from ARPES [2]. This flatness may lead to a van Hove-like singularity in the density of states.

The SVD method brings to this inversion problem a more rigorous and controlled approach than the maximum entropy technique. Contrary to previous findings the results of our calculations suggest that $U = 4t$ is in a regime in which the spectrum of quasiparticle (damped) excitations has a two-band structure, in spite of the on-site repulsion being sufficiently weak to allow substantial double occupancy. There is some support for the relevance of $U = 4t$ regime to high T_c superconductivity from a recent work by Beenen and Edwards [18].

We thank J. Jefferson, A. Bratkovsky, D. Edwards and P. Kornilovitch for stimulating discussions. This work was supported by SERC grant GR/J18675 and our general development of SVD techniques by the US Army Research Office, agreement no. DAAL03-92-G-0142.

References

1. K. Gofron *et al.*, *Phys. Rev. Lett.* **73**, 3302 (1994)
2. D.S. Dessau *et al.*, *Phys. Rev. Lett.* **71**, 2781 (1993);
D.M. King *et al.*, *Phys. Rev. Lett.* **73**, 3298 (1994).
3. P. Aebi *et al.*, *Phys. Rev. Lett.* **72**, 2757 (1994)
4. E. Dagotto, A. Nazarenko and M. Boninsegni, *Phys. Rev. Lett.* **73**, 728 (1994).
5. S. Haas, A. Moreo and E. Dagotto, *unpublished*.
6. A. Moreo, S. Haas, A. Sandvik and E. Dagotto, *unpublished*.
7. H.-B. Schüttler and D.J. Scalapino, *Phys. Rev.* **B34**, 4744 (1986).
8. S.R. White, *Phys. Rev.* **B44**, 4670 (1991);
M. Vekić and S.R. White, *Phys. Rev.* **B47**, 1160 (1993).
9. N. Bulut, D.J. Scalapino and S.R. White, *Phys. Rev. Lett.* **73**, 748 (1994).
10. S.R. White, *Phys. Rev.* **B46**, 5678 (1992).
11. E. Dagotto, *Rev. Mod. Phys.* **66**, 763 (1994).
12. G. Fano, F. Ortolani and A. Parola, *Phys. Rev.* **B46**, 1048 (1992)
13. N. Bulut, D.J. Scalapino and S.R. White, *Phys. Rev. Lett.* **72**, 705 (1994).
14. M. Bertero, C. De Mol and E.R. Pike, *Inverse Problems* **1**, 301 (1985);
M. Bertero and E.R. Pike, *Handbook of Statistics* **10**, *Eds. N.K. Bose and C.R. Rao*, Elsevier Science Publishers (1993).
15. M. Bertero, P. Branzi, E.R. Pike and L. Rebola, *Proc. R. Soc. London A* **415**, 257 (1988);
M. Bertero, C. De Mol and E.R. Pike, *Inverse Problems* **4**, 573 (1988).
16. M. Bertero, P. Boccacci and E.R. Pike, *Proc. R. Soc. London A* **383**, 15 (1982); **A 393**, 51 (1984);
M. Bertero, P. Branzi and E.R. Pike, *Proc. R. Soc. London A* **398**, 23 (1985).
17. M. Bertero and E.R. Pike, *Inverse Problems* **7**, 1 (1991); 21 (1991).
18. J. Beenen and D.M. Edwards, to be published in *Jour. of Low Temp. Phys.* .

Figure captions

Fig.1a: $A(\pi/2, \pi/2, \omega)$ for a 8^2 lattice. Solid line – SVD solution with infinite support, dotted line – SWF support is limited in the range [-8,8].

Fig.1b: $A(2\pi/5, 3\pi/5, \omega)$ for a 10^2 lattice. Solid line – SVD solution with infinite support, dotted line – SWF support is limited in the range [-8,8].

Fig.1c: $A(\pi/2, \pi/2, \omega)$ for a 12^2 lattice. Solid line – SVD solution with infinite support, dotted line – SWF support is limited in the range [-7,7].

Fig.2: Density of states as a function of ω .

Fig.3a: 8^2 lattice. Spectrum of single-particle excitations. Lower band – stars; upper band – circles. Dotted line – $\epsilon(\vec{k}) = -2t(\cos k_x + \cos k_y)$; solid line – $E(\vec{k})_{MF} = \pm \sqrt{\epsilon(\vec{k})^2 + \Delta^2}$. Points in the Brillouin zone: $\Gamma - (0, 0)$; $\bar{M} - (\frac{\pi}{2}, \frac{\pi}{2})$; $M - (\pi, \pi)$; $X - (\pi, 0)$.

Fig.3b: Same as (a) for a 12^2 lattice.

Fig. 1a

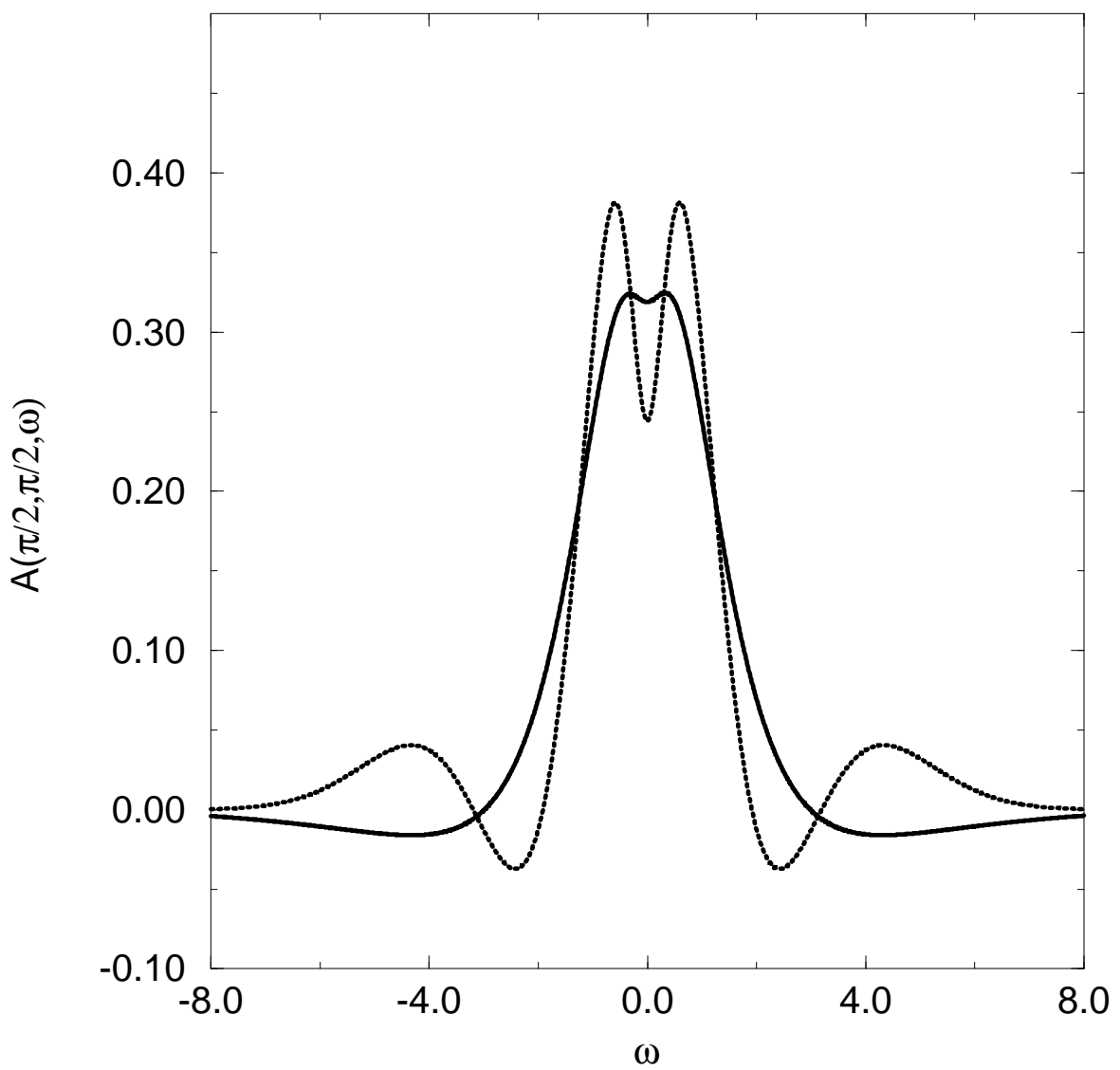


Fig. 1b

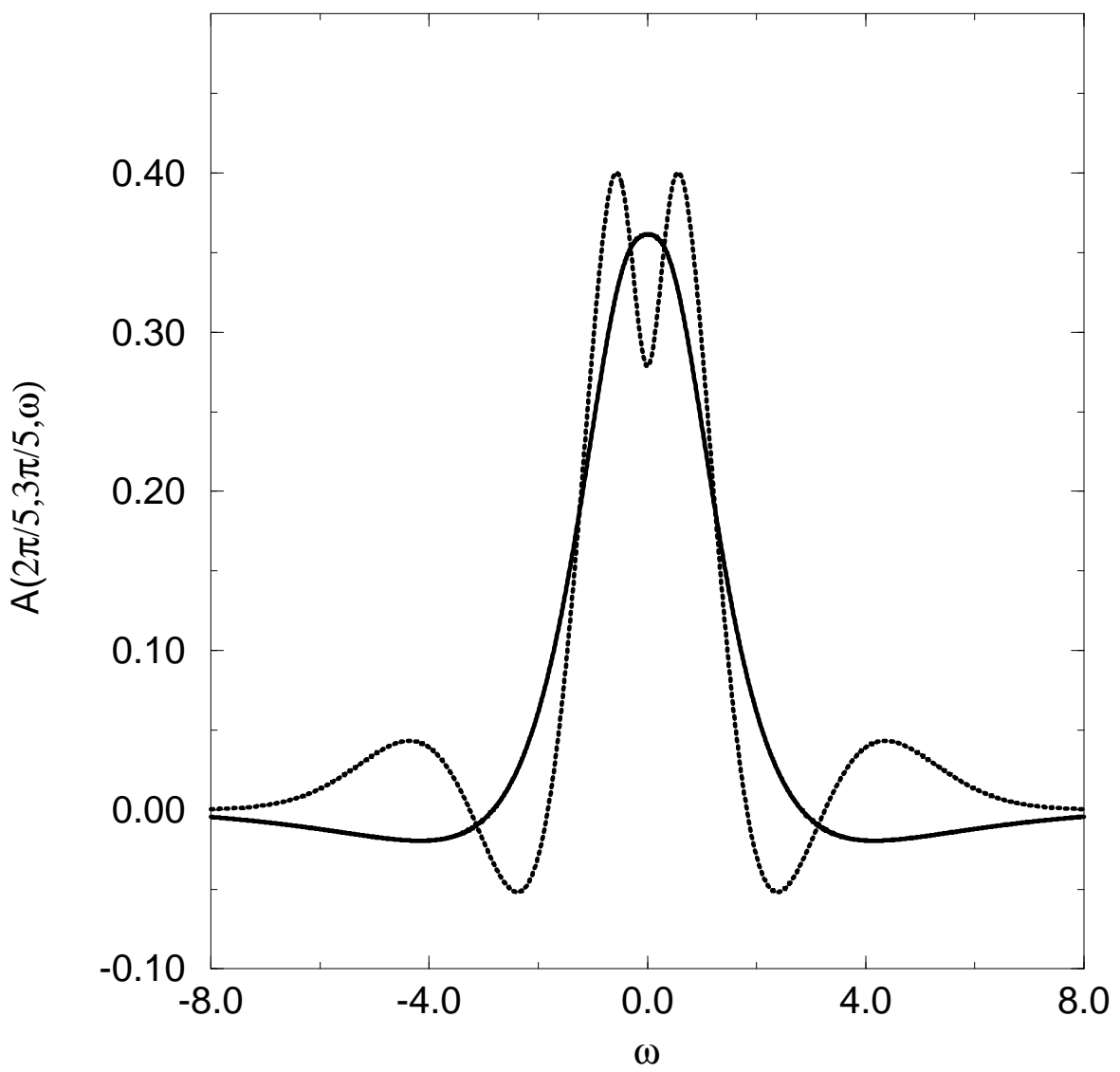


Fig. 1c

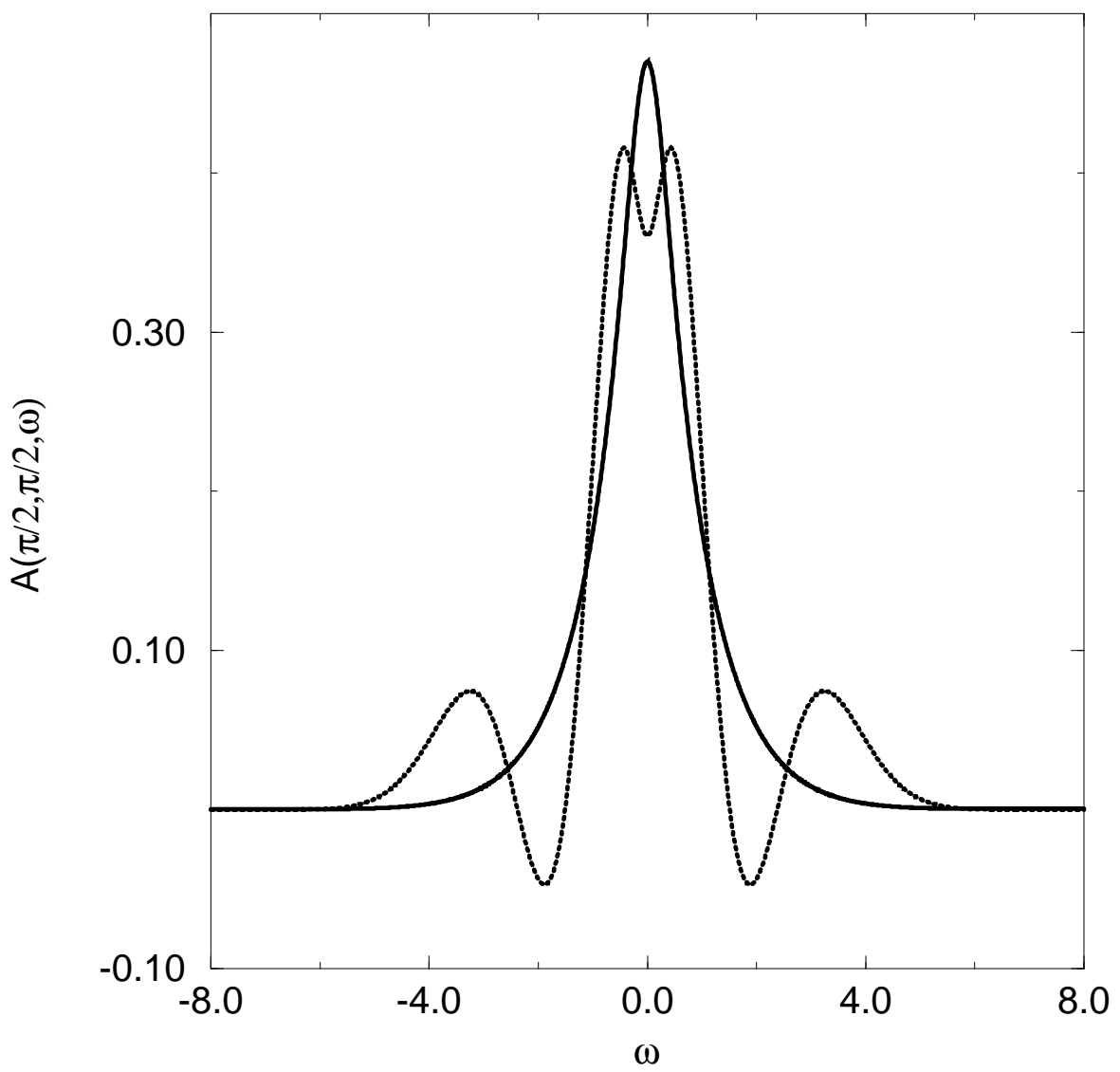


Fig.2

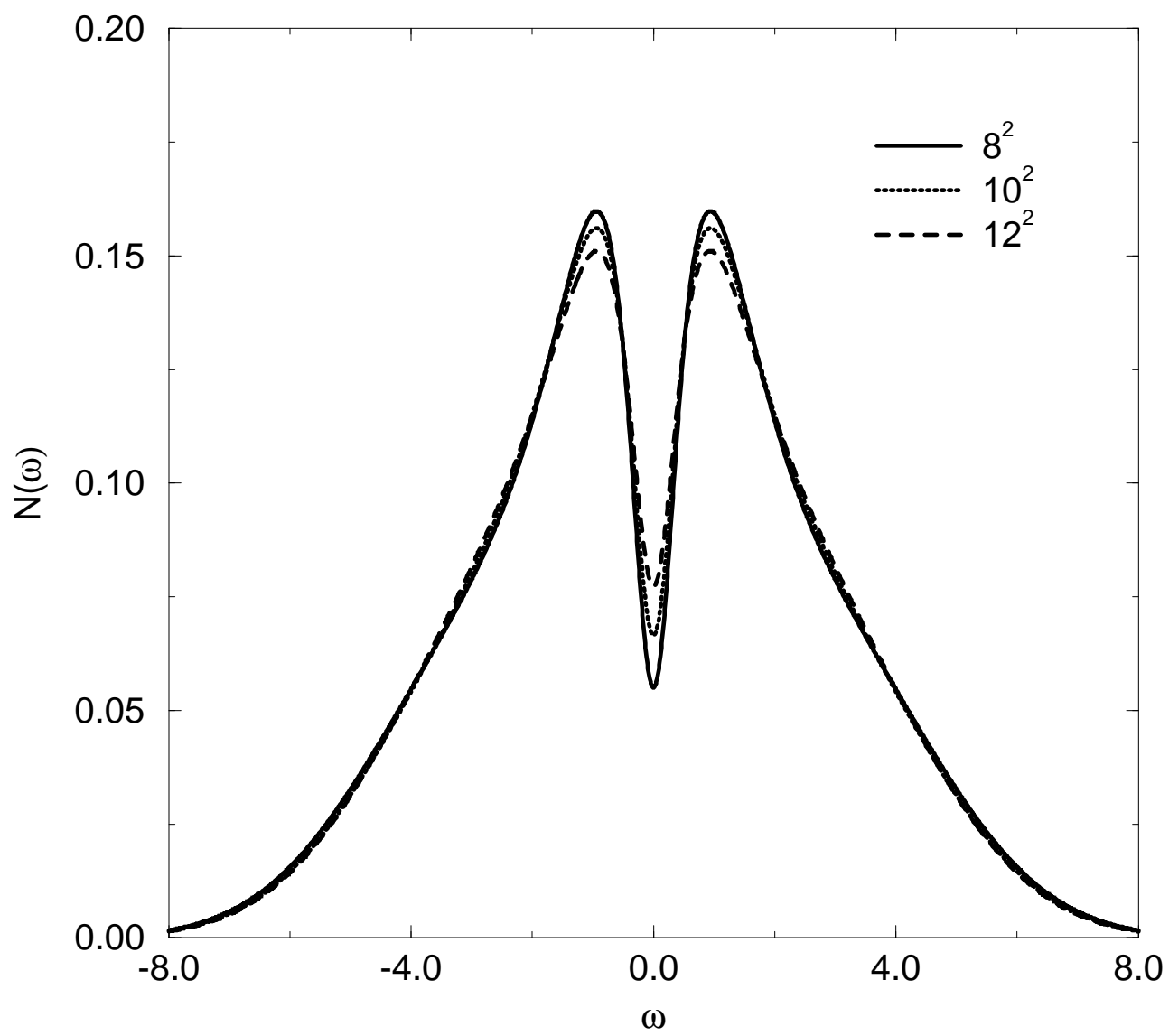


Fig.3a

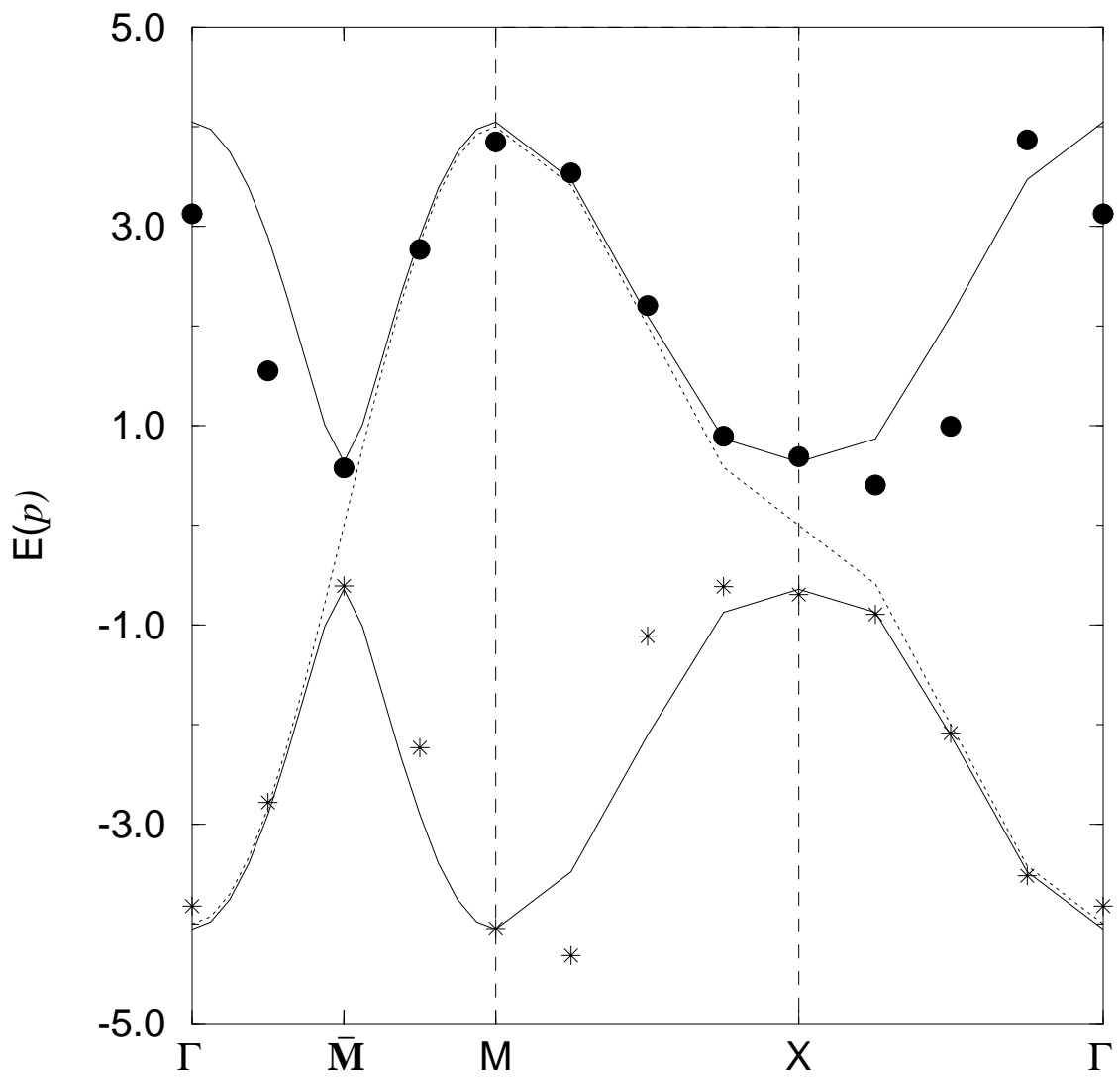


Fig. 3b

